Video-based Data Hiding by Exploring Prediction Error and Histogram Shifting

Alek Nur Fatman[1]   **Tohari Ahmad[1]***

[1]*Department of Informatics, Institut Teknologi Sepuluh Nopember, Indonesia*
* Corresponding author's Email: tohari@if.its.ac.id

Abstract: Information has been crucial in supporting daily activities. Many tasks must be accomplished by transferring not only public but also private information. This situation has brought the necessity for protecting it during transmission. Some mechanisms introduced, like data hiding, are still challenging, considering the quality of the data and the secret size can be protected. This research presents a reversible data hiding method for digital video based on prediction error and histogram shifting to approach those problems. There are six kinds of prediction errors used, three are created from two adjacent frames, and three are from a single frame. The selection of the shift location is determined by the histogram location, which has the highest peak point. The histogram is obtained by calculating the frequency of the subtraction of each value from its predicted value. The PSNR calculated from the stego and the original videos has an average of 73.45 dB. This value demonstrates that the proposed method outperforms the previous research.

Keywords: Data data hiding, Information security, Network security, Network infrastructure.

1. Introduction

Data confidentiality is getting more attention nowadays, where data exchange often occurs. Data hiding is one method that can approach this activity [1, 2]. In general, there are two kinds of data hiding, namely reversible data hiding (RDH) and irreversible hiding. RDH can extract the embedded data and recover the medium losslessly, which is useful for hiding sensitive information such as in the military, medical, legal, or something that requires no change in a media cover [3, 4]. Many RDH algorithms have been developed in various methods and applications, which are analyzed from different aspects, like in encrypted images [5], digital audio-based classification [6], trends of digital image-based data hiding [7], attack to cipher images [8], two-layer embedding [9], and predictor-based RDH [10]. In detail, the introduced methods include difference expansion (DE), histogram shifting (HS), and pixel value ordering (PVO), for various purposes, like file tampering detection [11] and watermarking [12]. Furthermore, RDH can be developed in various media, like image [7], audio [6], and video [13], with either spatial or frequency domain. For example,

multiple prediction error expansion [14], game-theoretic approach [15], and dual-images [16].

DE-based RDH method uses the difference between two pixels for its calculation. This difference value is multiplied by two then the zero-valued least significant bit (LSB) will be used for the embedding location. Differently, the HS method employs a histogram of all pixels as the embedding site. This histogram is created by finding the frequency where the value in each pixel appears. The HS method begins by shifting all pixels between the highest frequency (the peak point) and the lowest frequency (the zero point) towards the zero point by one bit. Confidential data can be embedded in pixels with the same value as the peak point. The weakness of HS is the large number of pixels that are shifted during the embedding process. The more pixels shifted, the worse the quality of the stego file.

In another study, Yeh et al. [17] developed the neighboring similarity (NS) method. They take advantage of the similarity of two adjacent frames in a video to create a prediction error. The similarity will increase the number of the same value in the prediction error. In this case, the greater frequency of the prediction error means the greater both the

frequency of the peak point and the number of payloads that can be embedded. The shifting process moves the histogram to the right towards the immense value in the prediction error. The number of changed pixels caused by this shifting is relatively big because values around the peak points in the histogram are considered high. This can be a drawback of this method, which should be overcome.

Concerning the number of values change during the shifting process, a scheme was developed [18] to determine the location and direction of the shift. This shift location can be done on the histogram created from the frame or the prediction error. The direction of the shift can also be done in three directions; it can be towards the lowest frequency, the lowest value, or the highest value. The selection is made by calculating the ratio between the peak point frequency and the number of shifted values. Overall, that research is to refine that in [17], even though it still has some spaces for improvement, considering the number of changed pixels during the shifting process.

Recently, a new high-fidelity RDH method, called pixel-based pixel value ordering (PPVO), has been proposed by Qu and Kim [10]. They use a collection of adjacent pixels (the context pixels) to make predictions. The embedding process can be carried out on a pixel with a value equal to the largest or smallest value of the context pixel. However, not all conditions meet the requirements, making the payload unable to be embedded into the cover. Consequently, the number of bits (payload) that can be protected in this scheme may not be adequate.

To increase the possibility of whether pixels can be embedded, a new scheme was developed by Ahmad and Fatman [19]. They take advantage of the similarity of values in the prediction error level two to increase the likelihood that the payload can be embedded. Nevertheless, their experimental results show that those values are not always more similar than those in level one. Furthermore, the similarity level of three sequential values in the prediction error is considered low, which affects the quality or imperceptibility.

It is shown that the use of prediction errors in the existing methods [10, 17-19] may not be optimal, depicted by their stego file quality. Furthermore, some recent video-based RDH research takes different views, such as compression [20] for hiding the data.

In this research, we improve the quality of the stego file by creating six prediction errors, three of which are created from two adjacent frames, and the other three are created from a single frame. The number of prediction errors can be used to find the embedding location to produce the best stego file.

The rest of this paper is organized as follows. Section 2 presents a brief review of some existing studies. Section 3 describes the proposed algorithm, which includes the embedding and extraction processes. The experimental results and analysis are shown in Section 4. Finally, Section 5 provides the conclusion.

2. Previous research

In this section, related research is reviewed. Here, research in [19] closely relates to this study, whose data embedding and extraction processes are presented.

The embedding stage starts with the creation of two-level prediction errors. In this case, prediction error level one is obtained by reducing the first frame's pixel value with the second frame's pixel value. The second level prediction error pes_i is created by reducing each value at the first level prediction error (pef_i) with the third next value (pef_{i+3}) based on Eq. (1).

$$pes_i = pef_i - pef_{i+3} \qquad (1)$$

The pixel changes are based on the previous two values, called predictive values (τ, β). In this research, τ denotes the predicted value with the most considerable value, and β is the smallest predictive value. The two predicted values are used to determine the direction of the pixel shift. The shift direction has three possible directions: to the right, away from the midpoint, and closer to the midpoint. The shift to the right is done when both predicted values have the same value; away from the midpoint is when the difference of the predicted values is one; closer to the midpoint is when the difference in the predicted values is more than one. The midpoint value (med) can be obtained based on Eq. (2).

$$med = \begin{cases} \frac{\tau+\beta}{2}, & \text{if } (\tau + \beta) \bmod 2 = 0 \\ \frac{\tau+\beta+1}{2}, & \text{if } (\tau + \beta) \bmod 2 = 1 \end{cases} \qquad (2)$$

The values in the prediction error level two are divided into several groups using Eq. (3).

The embedding process is carried out when the value is equal to the value of either τ or β. This embedding process is implemented according to Eq. (4).
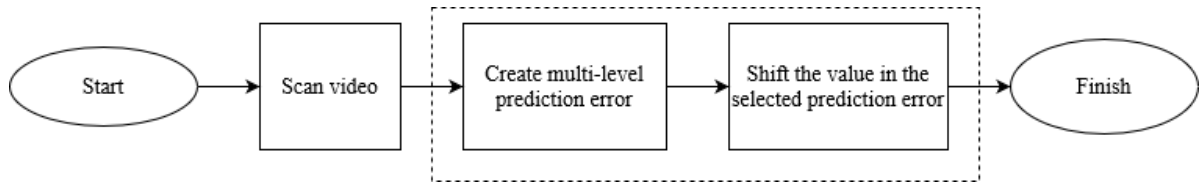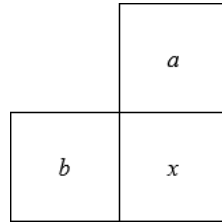
Figure. 1 The embedding process

Figure. 2 The predictive value

$$s1=\{a|a = \tau, \tau = \beta\}$$
$$s2=\{a|a > \tau, \tau = \beta\}$$
$$s3=\{a|a = \tau, \tau - \beta = 1\}$$
$$s4=\{a|a = \beta, \tau - \beta = 1\}$$
$$s5=\{a|a > \tau, \tau - \beta = 1\} \quad (3)$$
$$s6=\{a|a < \beta, \tau - \beta = 1\}$$
$$s7=\{a|a = \tau, \tau - \beta > 1\}$$
$$s8=\{a|a = \beta, \tau - \beta > 1\}$$
$$s9=\{a|a < \tau, a > med, \tau - \beta > 1\}$$
$$s10=\{a|a > \beta, a < med, \tau - \beta > 1\}$$

$$pes_i' = \begin{cases} pes_i + b, & \text{if } pes_i \in S1 \cup S3 \cup S8 \\ pes_i - b, & \text{if } pes_i \in S4 \cup S7 \\ pes_i + 1, & \text{if } pes_i \in S2 \cup S5 \cup S10 \\ pes_i - 1, & \text{if } pes_i \in S6 \cup S9 \\ pes_i, & \text{otherwise} \end{cases} \quad (4)$$

The original values equal to the midpoint or values that change to the same as the midpoint will be stored in the location map for use in the extraction process. The (+3)-th value in the first prediction error (pef_{i+3}) is obtained using Eq. (5).

$$pef_{i+3} = pef_i + pes_i' \quad (5)$$

The -th pixel value of the frame in the stego video (f_i) is obtained based on Eq. (6). To prevent it from underflow or overflow, the method changes f_i either from -1 to 0 or 256 to 255, stored in the location map.

$$f_i = f_{i-1} + pes_i \quad (6)$$

The steps in the extraction process are the same as those in the embedding process, except changing the values in the second-level prediction error. The payload value of this prediction error is obtained using Eq. (7).

$$b = \begin{cases} 0, & \text{if } pes_i = \tau \text{ or } pes_i = \beta \\ 1, & \text{if } pes_i = \tau + 1 \text{ and } |\tau - \beta| = 1 \\ 1, & \text{if } pes_i = \tau - 1 \text{ and } |\tau - \beta| > 1 \\ 1, & \text{if } pes_i = \beta + 1 \text{ and } |\tau - \beta| > 1 \end{cases} \quad (7)$$

For each pes_i whose value equals to the med, the algorithm subtracts one if the location map is one; and adds one if the location map is two. Next, shift the value in the second prediction error as in Eq. (8).

$$pes_i' = \begin{cases} pes_i - 1, & \text{if } pes_i \in S2 \cup S5 \cup S10 \\ pes_i + 1, & \text{if } pes_i \in S6 \cup S9 \\ pes_i, & \text{otherwise} \end{cases} \quad (8)$$

3. Proposed method

In this section, the embedding and extraction processes are explained. As previously described, this paper proposes an embedding method that improves several processes based on that in [19]. This change is illustrated by Fig. 1.

3.1 Embedding Process

The embedding process is done by creating a level one prediction error by subtracting all pixels from the frame with the pixel value of the next frame. Prediction error level two is created by subtracting all values in the prediction error level one with the following three values using Eq. (1). Furthermore, creating the third-level prediction error is done the same way, but it takes the value of the second-level prediction error, which will be deducted.

The prediction error is also created using the pixels in the second frame only as of the establishment's source. Taking the same method as forming the second level prediction error from the level one prediction error, this level one prediction error frame is created from the second frame. The

creation is also carried out to make a level two prediction error frame from the level one prediction error frame and level three prediction error frame from the level two prediction error frame. The number of prediction errors created is six, three from two adjacent frames and three from only one frame.

The next stage is the selection of the location of the shifting process. The location is determined by the predictive value of several prediction errors. There are two prediction values, namely the previous value and the previous third value, as illustrated in Fig. 2. The third value was chosen because the pixels from the video have three primary colors for each pixel, namely red, green, and blue.

Each value of each prediction error is to construct a histogram. Instead of calculating the frequency of each value, we take the frequency of the subtraction of each value from its predicted value. The shifting process is carried out on the prediction error, which has the peak point with the highest frequency.

The shift direction of the value in the selected prediction error is determined by the two predicted values (τ, β) and the peak point $(\dot{p})$ value. The values in the selected prediction error will be divided into several groups based on Eq. (3). The payload can insert the values in the prediction error if the value has the same value as one of the predicted values plus the peak point. The shifting process is carried out based on Eq. (9).

$$pes_i' = \begin{cases} pes_i + b, & \text{if } pes_i - \dot{p} \in S1 \cup S3 \cup S8 \\ pes_i - b, & \text{if } pes_i - \dot{p} \in S4 \cup S7 \\ pes_i + 1, & \text{if } pes_i - \dot{p} \in S2 \cup S5 \cup S10 \\ pes_i - 1, & \text{if } pes_i - \dot{p} \in S6 \cup S9 \\ pes_i, & \text{otherwise} \end{cases} \quad (9)$$

The value of the shift location, the peak point value, and the values that change to the midpoint value will be saved into the location map. Furthermore, this information will be used in the next step.

3.2 Extraction process

The extraction process begins by creating the selected prediction error in the same way as the embedding process. Then payload value is obtained based on Eq. (10).

$$b = \begin{cases} 0, & \text{if } pes_i - \dot{p} = \tau \text{ or } pes_i - \dot{p} = \beta \\ 1, & \text{if } pes_i - \dot{p} = \tau + 1 \text{ and } |\tau - \beta| = 1 \\ 1, & \text{if } pes_i - \dot{p} = \tau - 1 \text{ and } |\tau - \beta| > 1 \\ 1, & \text{if } pes_i - \dot{p} = \beta + 1 \text{ and } |\tau - \beta| > 1 \end{cases} \quad (10)$$

The next stage is the shifting process which is carried out based on Eq. (11).

$$pes_i' = \begin{cases} pes_i - 1, & \text{if } pes_i - \dot{p} \in S2 \cup S5 \cup S10 \\ pes_i + 1, & \text{if } pes_i - \dot{p} \in S6 \cup S9 \\ pes_i, & \text{otherwise} \end{cases} \quad (11)$$

4. Experiment results

The experiment was conducted using 15 videos as the cover taken from [21] and 11 payloads of different sizes, starting from 1 kb to 100 kb. These sizes represent various files in the actual application.

We first consider the impact of shifting locations. Tables 1 - 6 show the PSNR results from embedding with different shift locations. These tables show that the embedding performed using prediction error level one has the best stego video quality with an average PSNR value of 73.46 dB. The higher the level of prediction error used, the lower the quality of the stego video.

The same result happened to the prediction error frame. The higher the level of the prediction error frame, the lower the quality of the stego video. The embedding process using prediction error also has better stego video quality than using a prediction error frame.

Table 7 shows the PSNR value of the stego video using location selection. This table shows that most shift locations are carried out at prediction error level one. It can be seen from the PSNR value, which is mostly the same as the PSNR value from embedding using prediction error level one. Only a few embedding processes use shift locations in the level one prediction error frame; most of them are carried out at level one prediction error.

The results of the embedding PSNR using other methods were also used as a comparison, as depicted in Fig. 3. To make this comparison as fair as possible, we implement those methods, and evaluate them using same cover and payload data. Overall, it is depicted that increasing the payload size decreases the quality of the stego file. This pattern applies to all methods in the experiment. This figure shows the PSNR value from [17, 10, 19, 18]. The proposed method's PSNR value has slightly increased compared to [19] where the proposed method has an average PSNR of 73.45 dB while [19] is 73.04 dB. The improvement is significantly big compared to [17, 10], which have 70.43 dB and 69.07 dB, respectively. In a relatively small payload size, in this experiment is 1 kb, [18] generates the highest PSNR value. However, the increase of payload sizes causes

Table 1. PSNR of stego files obtained by the proposed method using prediction error level 1

Video	PSNR of Various Payload Sizes (dB) for each payload size (kb)										
	1	10	20	30	40	50	60	70	80	90	100
akiyo	86.18	80.67	78.18	76.62	75.43	74.54	73.75	73.13	72.51	71.98	71.55
bowing	86.51	81.55	78.62	76.92	75.62	74.69	73.89	73.24	72.68	72.13	71.69
car-phone	76.23	75.23	74.36	73.64	72.99	70.86	70.51	70.20	69.02	68.78	68.57
claire	78.73	77.17	75.96	75.04	74.27	73.67	72.24	71.83	71.46	71.08	70.78
coastguard	75.49	74.64	73.88	73.23	70.87	70.54	70.21	69.92	68.64	68.42	68.22
container	82.48	79.29	77.37	76.06	74.98	74.17	73.44	72.15	71.72	71.28	70.92
deadline	75.55	74.69	73.91	73.26	71.22	70.86	70.51	70.20	69.21	68.95	68.73
foreman	76.23	75.23	74.36	73.64	72.99	70.97	70.61	70.29	70.01	68.76	68.55
galleon	75.86	74.95	74.15	73.47	71.60	71.21	70.84	70.51	70.22	69.32	69.09
grandma	81.23	78.75	77.11	75.94	74.97	74.21	73.50	72.61	72.17	71.71	71.34
mother_daughter	80.22	78.09	76.56	75.45	74.51	73.79	73.14	72.17	71.75	71.31	70.94
pamphlet	78.04	76.76	75.56	74.64	73.83	73.19	72.04	71.60	71.23	70.83	70.50
paris	74.96	74.20	73.50	71.19	70.81	70.48	70.16	68.97	68.76	68.53	67.71
sign_irene	78.51	76.95	75.71	74.76	73.93	73.31	71.64	71.25	70.90	70.52	70.22
silent	84.82	80.26	77.94	76.45	75.28	74.41	73.65	73.04	72.21	71.72	71.31

Table 2. PSNR of stego files obtained by the proposed method using prediction error level 2

Video	PSNR of Various Payload Sizes (dB) for each payload size (kb)										
	1	10	20	30	40	50	60	70	80	90	100
akiyo	85.24	80.39	78.02	76.51	75.34	74.46	73.69	73.07	72.43	71.92	71.49
bowing	85.25	81.10	78.39	76.76	75.51	74.59	73.81	73.17	72.55	72.02	71.58
car-phone	75.64	74.76	73.97	73.31	70.81	70.48	70.16	69.87	68.65	68.42	68.22
claire	78.26	76.81	75.69	74.82	74.07	73.49	71.95	71.57	71.22	70.87	70.58
coastguard	74.84	74.09	73.41	72.83	70.42	70.12	69.82	68.43	68.25	68.04	67.08
container	81.36	78.72	76.99	75.78	74.76	73.98	73.29	71.83	71.43	71.02	70.68
deadline	75.18	74.38	73.65	73.04	70.90	70.56	70.23	69.94	68.89	68.66	68.45
foreman	75.80	74.88	74.07	73.40	71.04	70.69	70.35	70.05	68.73	68.50	68.31
galleon	75.36	74.54	73.80	73.17	71.18	70.83	70.48	70.18	69.16	68.91	68.69
grandma	80.11	78.09	76.65	75.57	74.68	73.96	73.28	72.31	71.90	71.47	71.12
mother_daughter	79.34	77.53	76.16	75.13	74.26	73.57	72.94	71.87	71.47	71.06	70.71
pamphlet	77.00	75.96	74.94	74.13	73.40	71.95	71.56	71.17	70.82	70.46	70.15
paris	74.78	74.05	73.37	71.00	70.63	70.32	68.99	68.78	68.57	68.35	67.52
sign_irene	77.93	76.54	75.40	74.50	73.72	73.16	71.36	70.99	70.66	70.31	70.05
silent	83.46	79.73	77.62	76.23	75.11	74.27	73.53	72.93	72.00	71.52	71.13

it to drop more dramatically than that of the proposed method. It also presents that the proposed method is more stable than others, considering the decline caused by the rise of the payload size. Additionally, the proposed method outperforms HEVC [20], which also carries out a compression technique.

Table 3. PSNR of stego files obtained by the proposed method using prediction error level 3

Video	PSNR of Various Payload Sizes (dB) for each payload size (kb)										
	1	10	20	30	40	50	60	70	80	90	100
akiyo	84.64	80.18	77.90	76.42	75.27	74.41	73.65	73.04	72.37	71.86	71.44
bowing	84.17	80.64	78.14	76.59	75.38	74.49	73.72	73.09	72.42	71.90	71.48
car-phone	75.25	74.44	73.70	73.08	70.58	70.26	68.82	68.61	68.41	67.54	67.38
claire	77.65	76.37	75.35	74.53	73.84	72.09	71.68	71.30	70.99	70.67	70.40
coastguard	74.70	73.98	73.32	70.62	70.29	68.73	68.51	68.31	67.26	67.10	66.28
container	80.97	78.51	76.85	75.67	74.68	73.91	73.23	71.68	71.30	70.90	70.56
deadline	74.78	74.04	73.36	70.98	70.61	70.29	69.07	68.85	68.64	68.42	67.62
foreman	75.54	74.68	73.90	73.25	70.84	70.51	70.18	68.76	68.56	68.34	67.33
galleon	75.11	74.33	73.62	71.32	70.94	70.60	70.27	69.14	68.93	68.69	68.49
grandma	79.08	77.43	76.14	75.19	74.37	73.67	72.49	72.04	71.67	71.26	70.92
mother_daughter	78.73	77.12	75.86	74.90	74.06	73.40	72.09	71.66	71.28	70.89	70.56
pamphlet	76.36	75.44	74.53	73.79	73.11	71.67	71.25	70.89	70.56	70.22	69.54
paris	74.50	73.80	71.07	70.72	70.37	68.96	68.73	68.52	67.61	67.43	67.28
sign_irene	77.44	76.18	75.12	74.28	73.53	71.52	71.11	70.76	70.44	70.13	69.13
silent	82.79	79.44	77.44	76.10	75.01	74.18	73.46	72.31	71.86	71.41	71.03

Table 4. PSNR of stego files obtained by the proposed method using prediction error frame level 1

Video	PSNR of Various Payload Sizes (dB) for each payload size (kb)										
	1	10	20	30	40	50	60	70	80	90	100
akiyo	75.81	74.91	74.11	73.43	71.09	70.74	70.40	70.10	68.87	68.64	68.44
bowing	77.19	75.98	74.96	74.15	73.42	71.52	71.11	70.76	70.44	70.11	69.11
car-phone	75.60	74.72	73.94	73.28	70.95	70.60	70.27	69.98	68.75	68.52	68.32
claire	77.01	75.86	74.88	74.10	73.43	71.46	71.07	70.73	70.43	69.33	69.08
coastguard	75.17	74.38	73.65	73.04	70.63	70.32	70.01	69.73	68.46	68.24	68.05
container	75.99	75.09	74.25	73.55	71.23	70.87	70.53	70.21	69.01	68.77	68.56
deadline	74.91	74.15	73.46	70.78	70.43	68.90	68.67	67.59	67.44	66.59	66.46
foreman	75.13	74.36	73.63	73.02	70.60	70.29	69.98	68.63	68.43	68.22	67.27
galleon	75.16	74.43	73.70	71.02	70.68	70.36	68.91	68.70	68.50	67.50	67.35
grandma	75.54	74.70	73.96	73.31	70.92	70.59	70.27	68.94	68.74	68.52	67.58
mother_daughter	75.45	74.60	73.84	73.21	70.83	70.50	70.18	68.84	68.64	68.42	68.22
pamphlet	75.90	74.97	74.15	73.46	72.83	70.77	70.43	70.12	69.85	68.67	68.46
paris	74.55	73.85	70.85	69.10	68.86	67.67	66.72	66.59	65.84	65.19	64.64
sign_irene	75.43	74.58	73.82	73.20	70.83	70.49	70.17	68.84	68.63	68.41	67.48
silent	74.86	74.13	73.44	70.76	70.41	68.87	68.65	68.45	67.41	67.24	66.44

It can be inferred that changing the prediction value from the previous two values to the previous value and the previous three values can improve the quality of the stego video. It can be proven as shown in Fig. 3. In the case of the method [19], it is because they use level two prediction error as the shift location. The graph also depicts that [19] and the proposed method have almost similar characteristics. Furthermore, the proposed method can steadily improve [19].

Table 5. PSNR of stego files obtained by the proposed method using prediction error frame level 2

Video	PSNR of Various Payload Sizes (dB) for each payload size (kb)										
	1	10	20	30	40	50	60	70	80	90	100
akiyo	75.22	74.43	73.70	73.08	70.69	70.37	70.05	68.71	68.51	68.30	67.35
bowing	76.51	75.46	74.55	73.80	73.12	71.14	70.77	70.44	70.14	69.00	68.78
car-phone	75.08	74.29	73.58	72.97	70.57	70.25	69.95	68.61	68.41	68.20	67.27
claire	76.29	75.29	74.42	73.72	71.42	71.04	70.68	70.37	69.18	68.93	68.71
coastguard	74.73	74.00	73.33	70.67	70.33	70.03	68.58	68.38	68.19	67.17	67.02
container	75.43	74.63	73.86	73.21	70.84	70.50	70.18	68.85	68.64	68.42	67.48
deadline	74.48	73.79	73.15	70.44	70.12	68.57	68.36	67.26	67.12	66.26	66.14
foreman	74.66	73.96	73.29	70.59	70.27	69.97	68.50	68.30	68.12	67.10	66.95
galleon	74.74	74.05	73.38	70.71	70.37	68.81	68.60	68.40	67.37	67.20	66.38
grandma	75.24	74.45	73.74	71.07	70.71	70.40	68.95	68.74	68.55	67.54	67.39
mother_daughter	74.92	74.16	73.46	70.80	70.45	70.14	68.68	68.48	68.29	67.27	67.12
pamphlet	75.29	74.48	73.73	73.10	70.72	70.39	70.07	68.73	68.53	68.31	68.12
paris	74.31	73.65	70.63	70.31	68.66	67.47	67.30	66.39	66.28	65.53	64.91
sign_irene	74.95	74.19	73.49	70.84	70.49	70.18	68.74	68.53	68.34	67.33	67.18
silent	74.54	73.85	73.20	70.51	70.19	68.64	68.42	68.23	67.18	67.02	66.21

Table 6. PSNR of stego files obtained by the proposed method using prediction error frame level 3

Video	PSNR of Various Payload Sizes (dB) for each payload size (kb)										
	1	10	20	30	40	50	60	70	80	90	100
akiyo	75.15	74.37	73.64	70.99	70.63	69.10	68.87	68.65	67.63	67.46	66.65
bowing	76.41	75.38	74.48	73.74	71.47	71.08	70.71	70.39	69.21	68.95	68.73
car-phone	74.92	74.16	73.46	70.80	70.45	68.93	68.70	68.50	67.48	67.31	66.51
claire	76.34	75.34	74.47	73.79	71.44	71.07	70.73	69.44	69.21	68.97	68.06
coastguard	74.83	74.09	73.41	70.75	70.40	68.87	68.65	68.44	67.40	67.24	66.42
container	75.24	74.47	73.72	71.06	70.70	69.17	68.94	68.72	67.70	67.52	66.72
deadline	74.72	73.99	70.96	69.21	67.96	66.99	66.84	66.07	65.42	64.84	64.34
foreman	74.60	73.90	70.90	70.57	68.90	68.69	67.54	67.38	66.51	66.37	65.66
galleon	74.84	74.14	71.12	70.78	69.12	68.89	67.74	67.57	66.70	65.96	65.85
grandma	75.16	74.39	73.68	71.00	70.65	69.13	68.90	67.82	67.66	66.81	66.68
mother_daughter	74.83	74.08	73.40	70.71	70.37	68.83	68.60	67.52	67.36	66.51	66.38
pamphlet	75.16	74.37	73.64	70.99	70.63	70.31	68.86	68.65	68.45	67.45	67.29
paris	74.61	71.28	69.40	68.09	66.39	65.69	64.64	64.15	63.73	63.03	62.69
sign_irene	75.01	74.24	73.56	70.89	70.54	69.01	68.78	67.71	67.55	66.70	66.57
silent	74.66	73.95	70.95	70.61	68.95	67.76	67.59	66.69	65.95	65.83	65.21

5. Conclusion

The method proposed in this paper develops a technique that uses six prediction errors. Three of which are created from two adjacent frames, and the other three are created from a single frame. The stego video quality of the proposed method has improved when compared to previous research. The best stego

Table 7. PSNR of stego files obtained by the proposed method using location selection

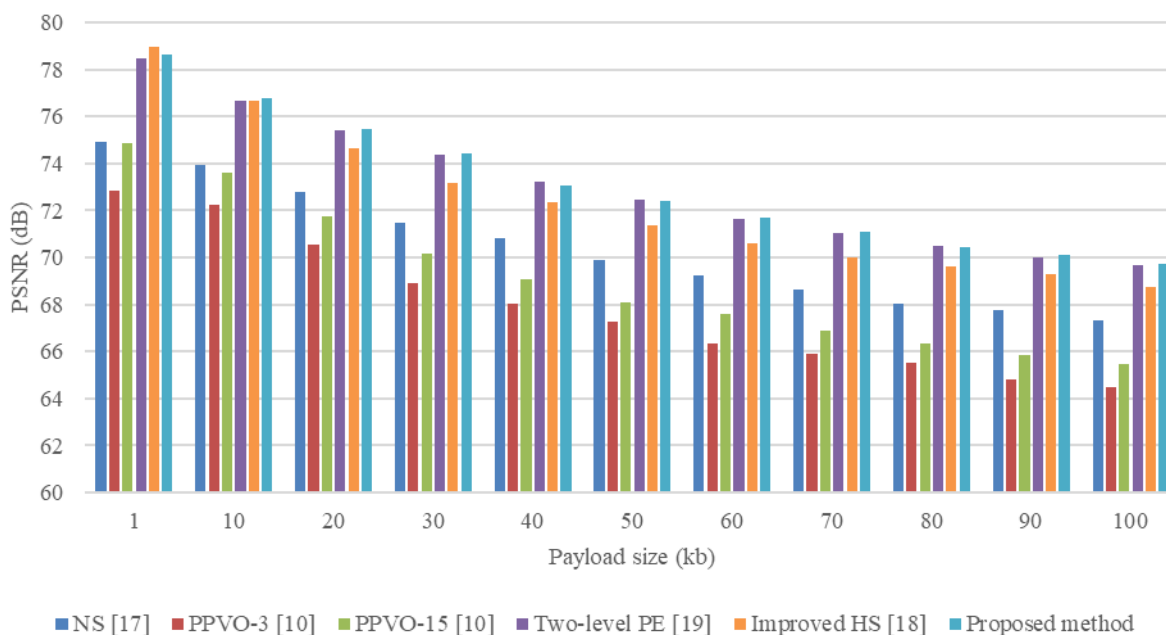| Video	PSNR of Various Payload Sizes (dB) for each payload size (kb)										
	1	10	20	30	40	50	60	70	80	90	100
akiyo	86.18	80.67	78.18	76.62	75.43	74.54	73.75	73.13	72.51	71.98	71.55
bowing	86.51	81.55	78.62	76.92	75.62	74.69	73.89	73.24	72.68	72.13	71.69
car-phone	76.23	75.23	74.36	73.64	72.99	70.79	70.45	70.14	68.98	68.74	68.53
claire	78.73	77.17	75.96	75.04	74.27	73.67	72.24	71.83	71.46	71.08	70.78
coastguard	75.49	74.64	73.88	73.23	70.87	70.54	70.21	69.92	68.64	68.42	68.22
container	82.48	79.29	77.37	76.06	74.98	74.17	73.44	72.15	71.72	71.28	70.92
deadline	75.55	74.69	73.91	73.26	71.22	70.86	70.51	70.20	69.21	68.95	68.73
foreman	76.23	75.23	74.36	73.64	72.99	70.97	70.61	70.29	70.01	68.76	68.55
galleon	75.86	74.95	74.15	73.47	71.60	71.21	70.84	70.51	70.22	69.32	69.09
grandma	81.23	78.75	77.11	75.94	74.97	74.21	73.50	72.61	72.17	71.71	71.34
mother_daughter	80.22	78.09	76.56	75.45	74.51	73.79	73.14	72.17	71.75	71.31	70.94
pamphlet	78.04	76.76	75.56	74.64	73.83	73.19	72.04	71.60	71.23	70.83	70.50
paris	74.96	74.20	73.50	71.19	70.81	70.48	70.16	68.97	68.76	68.53	67.71
sign_irene	78.51	76.95	75.71	74.76	73.93	73.31	71.64	71.25	70.90	70.52	70.22
silent	84.82	80.26	77.94	76.45	75.28	74.41	73.65	73.04	72.21	71.72	71.31

Figure. 3 PNSR values of the proposed method and the previous research

video quality is obtained when the shift location is at prediction error level one.

For further research, it is possible to determine the method for making prediction errors and the embedding process so that fewer pixels change. As the number of changing pixels decreases, the quality of the stego file will increase.

Conflicts of Interest

The authors declare no conflict of interest.

Author Contributions

Conceptualization, ANF and TA; methodology, ANF and TA; software, ANF; validation, ANF; formal analysis, ANF and TA; investigation, ANF; resources, ANF; data curation, ANF; writing—original draft preparation, ANF; writing—review and editing, ANF and TA; visualization, ANF; supervision, TA; project administration, TA; funding acquisition, TA.

References

[1] X. Wu, T. Qiao, M. Xu, and N. Zheng, "Secure reversible data hiding in encrypted images based on adaptive prediction-error labeling", *Signal Processing*, Vol. 188, p. 108200, 2021.

[2] L. Rakhmawati, S. Suwadi, and W. Wirawan, "Blind robust and self-embedding fragile image watermarking for image authentication and copyright protection with recovery capability", *International Journal of Intelligent Engineering and Systems*, Vol. 13, No. 5, pp. 197-210, 2020.

[3] X. Chen and C. Hong, "An Efficient Dual-image Reversible Data Hiding Scheme Based on Exploiting Modification Direction", *J. Inf. Secur. Appl.*, Vol. 58, p. 102702, 2021.

[4] A. Benhfid, E. B. Ameur, and Y. Taouil, "Reversible steganographic method based on interpolation by bivariate linear box-spline on the three directional mesh", *J. King Saud Univ. - Comput. Inf. Sci.*, Vol. 32, No. 7, pp. 850-859, 2020.

[5] P. Puteaux, S. Y. Ong, K. S. Wong, and W. Puech, "A survey of reversible data hiding in encrypted images - The first 12 years", *J. Vis. Commun. Image Represent.*, Vol. 77, No. September 2020, p. 103085, 2021.

[6] A. A. Alsabhany, A. H. Ali, F. Ridzuan, A. H. Azni, and M. R. Mokhtar, "Digital audio steganography: Systematic review, classification, and analysis of the current state of the art", *Comput. Sci. Rev.*, Vol. 38, p. 100316, 2020.

[7] I. J. Kadhim, P. Premaratne, P. J. Vial, and B. Halloran, "Comprehensive survey of image steganography: Techniques, Evaluations, and trends in future research", *Neurocomputing*, Vol. 335, pp. 299-326, 2019.

[8] C. Li, Y. Zhang, and E. Y. Xie, "When an attacker meets a cipher-image in 2018: A Year in Review", *J. Inf. Secur. Appl.*, Vol. 48, pp. 1-9, 2019.

[9] C. Lee, J. Shen, Y. Wu, and S. Agrawal, "PVO-Based Reversible Data Hiding Exploiting Two-Layer Embedding for Enhancing Image Fidelity", *Symmetry (Basel).*, Vol. 12, No. 7, p. 1164, 2020.

[10] X. Qu and H. J. Kim, "Pixel-based pixel value ordering predictor for high-fidelity reversible data hiding", *Signal Processing*, Vol. 111, pp. 249-260, 2015.

[11] L. Rakhmawati, T. Suryani, W. Wirawan, S. Suwadi, and E. Endroyono, "Exploiting self-embedding fragile watermarking method for image tamper detection and recovery", *International Journal of Intelligent Engineering and Systems*, Vol. 12, No. 4, pp. 62-70, 2019.

[12] S. Jiao, C. Zhou, Y. Shi, W. Zou, and X. Li, "Review on optical image hiding and watermarking techniques", *Opt. Laser Technol.*, Vol. 109, No. January 2018, pp. 370-380, 2019.

[13] Y. Liu, S. Liu, Y. Wang, H. Zhao, and S. Liu, "Video steganography: A review", *Neurocomputing*, Vol. 335, pp. 238-250, 2019.

[14] Y. Bai, G. Jiang, Z. Zhu, H. Xu, and Y. Song, "Reversible data hiding scheme for high dynamic range images based on multiple prediction error expansion", *Signal Process. Image Commun.*, Vol. 91, No. December 2020, p. 116084, 2021.

[15] S. Kumar and R. Soundrapandiyan, "A multi-image hiding technique in dilated video regions based on cooperative game-theoretic approach", *J. King Saud Univ. - Comput. Inf. Sci.*, No. in press, available online 18 June 2021, 2021.

[16] H. Yao, F. Mao, C. Qin, and Z. Tang, "Dual-JPEG-image reversible data hiding", *Inf. Sci. (Ny).*, Vol. 563, pp. 130-149, 2021.

[17] H. L. Yeh, S. T. Gue, P. Tsai, and W. K. Shih, "Reversible video data hiding using neighbouring similarity", *IET Signal Process.*, Vol. 8, No. 6, pp. 579-587, 2014.

[18] T. Ahmad and A. N. Fatman, "Improving the performance of histogram-based data hiding method in the video environment", *J. King Saud Univ. - Comput. Inf. Sci.*, No. in press, available on line 22 April 2020, 2020.

[19] A. N. Fatman and T. Ahmad, "Two Level Prediction Error and Three Direction Shifting for Hiding Data in Digital Video", In: *Proc. of International Seminar on Intelligent Technology and Its Applications*, 2021.

[20] J. Vivek and B. Gadgay, "Video Steganography Using Chaos Encryption Algorithm with High Efficiency Video Coding for Data Hiding", *International Journal of Intelligent Engineering and Systems*, Vol. 14, No. 5, pp. 15-24, 2021.

[21] "Video Test Media", *Xiph.org Video Test Media [derf's collection]*. [Online]. Available: https://media.xiph.org/video/derf/. [Accessed: 10-Nov-2019].